J. Membrane Biol. 161, 93–104 (1998)

The Journal of
Membrane
Biology



# Regulation of the MDCK Cell Tight Junction

**O.N. Kovbasnjuk, U. Szmulowicz, K.R. Spring**

Laboratory of Kidney and Electrolyte Metabolism, National Heart Lung and Blood Institute, National Institutes of Health, Building 10, Room 6N260, Bethesda, MD 20892-1603, USA

Received: 17 June 1997/Revised: 28 August 1997

**Abstract.** The sodium flux across individual tight junctions (TJ) of low-resistance MDCK cell monolayers grown on glass coverslips was determined as a measure of paracellular permeability. Increases in perfusate glucose concentration from 5 to 25 mM decreased tight junction Na permeability. This permeability decrease was not specific as nonmetabolizable analogues of glucose caused similar diminutions in TJ Na permeability. Stimulation of protein kinase A increased TJ Na permeability, and inhibition of protein kinase A decreased TJ Na permeability. Transepithelial electrical resistance of monolayers grown on permeable supports did not change as predicted from the observed alterations in TJ Na permeability of monolayers grown on glass coverslips. Fluorescent labeling of cell F-actin showed that increased F-actin in the perijunctional ring correlated with higher TJ Na permeability. Although a low dose of cytochalasin D did not change TJ Na permeability, it disrupted the cytoskeleton and blocked the decrease in TJ Na permeability caused by glucose. Cytochalasin D failed to block the effects of protein kinase A stimulation or inhibition on TJ Na permeability. We conclude that tight junction sodium permeability is regulated both by protein kinase A activity and by other processes involving the actin cytoskeleton.

**Key words:** Glucose — Protein kinase A — Cytoskeleton — Sodium permeability — Transepithelial electrical resistance — Phalloidin — Cytochalasin D

## Introduction

Epithelial tight junctions (TJ) form a selectively permeable and regulated barrier to paracellular fluid, ion and molecule diffusion (Diamond, 1977; Cereijido, 1992). Tight junctional permeability may vary widely either in different epithelia or in response to a variety of physiological, pharmacological and pathological conditions (Gumbiner, 1987; Balda, 1992). A correlation between the structure of the TJ and its permeability, particularly to large electron-dense tracers, has been made from observation of the number of parallel strands of the TJ seen in freeze-fracture replicas (Claude, 1978; Schneeberger & Lynch, 1992).

Many factors have been reported to alter TJ permeability. All the classical second messengers including $Ca^{2+}$, adenosine 3′,5′-cyclic monophosphate (cAMP), G proteins, protein kinase C are said to influence the barrier properties of the TJ (Balda, 1992; Anderson & van Italie, 1995; Stevenson & Begg, 1994). However, the effects vary among epithelia suggesting that different regulatory mechanisms are involved or predominate in different cell types. Methodological concerns have also resulted in confusion about the evidence for regulation of TJ permeability. For example, the first paper to describe alterations in TJ permeability showed that the transepithelial electrical resistance (TER) of *Necturus* gallbladder was slowly increased by addition of cAMP (Duffey et al., 1981). Recent investigations (Kottra, Haase & Frömter, 1993; Kottra & Frömter, 1993) concluded that no change in *Necturus* gallbladder TJ permeability actually occurred in response to cAMP addition and that the observed increase in TER was due to a collapse of the lateral intercellular spaces (LIS). Other studies on intestinal epithelia (Bakker & Groot, 1984, 1989; Holman et al., 1979) and MDCK cells (Balda et al., 1991) reported that cAMP addition reduced TER, a result consistent with an increase in TJ permeability. We recently described a measurement technique for the determination of the sodium permeability of an individual MDCK cell tight junction and showed that a cAMP analogue rapidly

*Correspondence to:* O.N. Kovbasnjuk

and reversibly increased TJ sodium permeability (Kovbasnjuk et al., 1995).

It has been reported that the presence of glucose in the small intestinal lumen increased the paracellular Na and mannitol permeability and decreased both the TER and the number of junctional strands (Madara & Pappenheimer, 1987; Atisook, Carlson & Madara, 1990). An apparent association between small intestinal TJ permeability and cytoskeletal actin filaments resulted in the proposal that the perijunctional cytoskeleton may regulate transjunctional permeability (Madara & Pappenheimer, 1987; Madara et al., 1988; Madara, 1991; Stevenson & Begg, 1994).

In the present study, we utilized our method for the direct measurement of the Na flux across a localized region of the tight junction of low-resistance MDCK epithelial cells (Kovbasnjuk et al., 1995) to examine the regulation of TJ Na permeability in the presence of glucose and glucose analogues. We found that an increased glucose concentration resulted in a large decrease in the TJ Na permeability and that the glucose-induced decrease in TJ Na permeability was prevented by a low dose of cytochalasin D, that did not, by itself, change the Na flux across the TJ. Transepithelial electrical resistance (TER) of MDCK monolayers grown on permeable supports did not correlate with most of the changes in TJ Na permeability revealed from the sodium fluxes measured on monolayers grown on glass coverslips. We also performed a quantitative analysis of the alterations in the distribution of actin filaments (F-actin) in the perijunctional actin-myosin ring to discern any relationship between TJ Na permeability and the cytoskeleton. Our results showed that treatment with cAMP analogues, glucose, or cytochalasin D changed the total amount of F-actin, rather than its distribution, and that the changes in TJ Na permeability caused by cAMP analogues and glucose displayed an apparent correlation with the total quantity of F-actin in the perijunctional actin-myosin ring such that increases in transjunctional Na permeability corresponded to higher amounts of F-actin.

## Materials and Methods

### Cell Culture

Low-resistance MDCK cells, passages 68–76 from the American Type Culture Collection (Rockville, MD), were cultured as previously described (Harris et al., 1994) using Dulbecco's modified Eagle medium (DMEM) with 10% fetal bovine serum (Gibco, Grand Island, NY) and 2 mM glutamine without added riboflavin, antibiotics and phenol red. For experimental purposes the cells were grown on glass coverslips or on filters (Anocell, Whatman, Clifton, NJ) and were used after 6–11 days.

### Experimental Solutions

The isotonic experimental solutions were (in mM): *control*—142 Na, 5.3 K, 1.8 Ca, 0.8 Mg, 126.9 Cl, 0.8 $SO_4$, 24 $HCO_3$, 5.6 glucose; *low Na*—24 NaCl plus 118 LiCl as a NaCl replacement; *high glucose*—same as control except that Na reduced to 130, Cl to 114.9, and glucose increased to 25; *high glucose, low Na*—24 NaCl with 106 LiCl as a NaCl replacement, glucose 25. The osmolarity of all solutions was 292–298 mOsm/kg; the pH was adjusted to 7.4 at 37°C after they were gassed with 5% $CO_2$/95% air. The *hypertonic* solutions were the same composition as a high glucose solution with high or low Na except that 25 raffinose was added to give an osmolarity of 329–336 mOsm/kg.

### Perfusion System

For the Na flux measurements, monolayers were grown on cover slips and the apical surface was perfused with experimental solutions in a closed chamber as described in Harris et al. (1994). The perfusion solution was switched rapidly by computer-controlled pinch valves.

### Chemicals

SBFO (sodium-binding benzofuran oxazole ammonium salt) was obtained from Molecular Probes (Eugene, OR). Sp-cAMPS ($S_p$-Adenosine cyclic 3′,5′-phosphorothioate) and Rp-cAMPS ($R_p$-Adenosine cyclic 3′,5′-phosphorothioate) were purchased from BioLog (La Jolla, CA). Cytochalasin D, α-methyl-D-glucoside and 3-O-methyl-D-glucose were purchased from Sigma (St. Louis, MO). Raffinose was from Baker (Phillipsburg, NJ).

### Fluorescence Microscopy

The experiments were performed on the stage of an upright microscope (Ortholux II, Leica, Deerfield, IL) equipped for bright field and low light level fluorescence (Chatton & Spring, 1993). Epifluorescence illumination was achieved using a dual path 75 W xenon lamp assembly (Model 60000, Oriel, Stratford, CT) equipped with 10 nm bandpass 340 nm and 380 nm filters (Omega Optical, Brattleboro, VT). Switching the wavelength between 340 nm and 380 nm was done by opening and closing fast shutters (Uniblitz, Vincent Associates, Rochester, NY). The light source was connected to the microscope by means of a fused silica optical fiber (C Technologies, Verona, NJ). The fluorescence filter cube contained a 400 nm dichroic mirror and a 430 nm barrier filter. Bright field imaging was achieved with a 50W tungsten halogen lamp (Leica).

The monolayers were observed through a 100×/1.3 N.A. objective lens (Nikon, Melville, NY), using a microchannel plate intensifier (KS-1381, Video Scope, Washington, D.C.) and video camera (VS-2000N, Video Scope). An 8-frame running average was used to reduce the noise level of the image (LKH 9000, Video Scope) which was stored on an optical memory disc recorder (OMDR, TQ-2028F, Panasonic, Newark, NJ) for later offline analysis. The sequence of events (e.g., solution valves, intensifier gain, illumination shutters, stepper motor) during the experiment was controlled by a computer using a custom-made program.

### SBFO Loading into the LIS

To incorporate fluorescent dye into the LIS, we used the approach described previously (Chatton & Spring, 1995). Briefly, the cell monolayers were incubated in their culture dish for 70–80 min with the free acid SBFO (~250 μM in buffered experimental solutions with 142 Na). During the incubation period, the SBFO molecules passively diffused across the tight junctions and progressively filled the LIS compartment and the domes. After washout of the fluorescence dye from the bathing

solution, the SBFO trapped in the LIS allowed measurements for up to 60 min until the signal-to-noise ratio diminished because of back diffusion of the dye through the TJ.

### Image Analysis

Images were transferred from the optical disc recorder to an image analysis workstation and analyzed as described previously (Chatton & Spring, 1995). Briefly, segmentation of the bright LIS and dark cellular regions of the 380 nm image was achieved from a binary image after thresholding. Regions of the LIS separated by small intensity differences were connected to each other by repeated dilation and erosion of the binary image, and the same outline of the LIS was used as a template for both 340 nm and 380 nm images. A ratio of the mean pixel intensity of the area inside the template of the two images was used as a measurement of Na concentration.

### Localization of F-actin

The procedure for staining F-actin with phalloidin followed that of (Mills & Lubin, 1986). Cells grown on coverslips in Petri dishes were washed twice with 2 ml of 37°C bicarbonate Ringer equilibrated with 95% room air—5% $CO_2$; 2 ml of experimental solutions were added, and the cells were allowed to equilibrate in a 5% $CO_2$ incubator at 37°C. At the end of the appropriate experimental period, formaldehyde was added to a final concentration of 3.7%, and fixation was continued for 25 min. The coverslips were then washed twice in phosphate-buffered saline (PBS) for 5 min., extracted in acetone at −20°C for 5 min, air dried, and placed in individual plastic dishes. Each coverslip was covered with 1 ml of the dye solution (10 μl of a stock solution of 300 units of Oregon-Green-488-phalloidin dissolved in 1 ml of PBS) for 1 hr at room temperature and then washed twice for 5 min in PBS and mounted on a glass slide in a 1:1 PBS-glycerol solution.

### Confocal Fluorescence Microscopy

Actin filament distribution was analyzed from confocal images of the fluorescently labeled polymerized actin (F-actin). The cells were illuminated with low light at 488 nm and optical sections of the monolayers were obtained at 0.5 μm intervals from the basal to the apical surface. The experiments were performed on the stage of an inverted microscope (Diaphot, Nikon, Melville, NY) equipped with a video-rate confocal attachment (Odyssey, Noran, Middleton, WI). The cell monolayers were observed with a 100×/1.32 N.A. objective lens (Nikon). The images were stored on disk for subsequent analysis. Each image was the average of 64 video frames. The sequence of events (e.g., video gain, illumination intensity, stepper motor) during the experiment was controlled by a computer using commercial software (Image-1, Universal Imaging, West Chester, PA).

### Analysis of Confocal Fluorescence Microscopy Images

Several steps were required to measure the intensity of the fluorescence of actin filaments using Image-1 software. Two or three cells were selected for analysis from each image of the apical surface of the monolayers. Two image masks for each cell, representing the bright actin ring around the cell and the darker intracellular area, were generated by thresholding the fluorescent image to define the measurement regions of interest. The average of intensity within the region bounded by the mask was calculated. Correction for the corresponding photomultiplier gain was applied for every experiment.

### Deblurring of F-actin Confocal Images

The confocal fluorescence images were still somewhat blurred by out-of-focus light that reduced image contrast and that could cause errors in the quantitation of intensity values. To determine the magnitude of such errors, we digitally deblurred several series of images of F-actin distribution using the Exhaustive Photon Reassignment algorithm (Scanalytics, Billerica, MA). The intensities of the perijunctional actin-myosin ring and terminal web regions of the deblurred images, defined from the masks on the thresholded images, were analyzed in the same fashion as described above. While quantitation of F-actin filaments in deblurred images demonstrated a higher intensity in the perijunctional ring and lower in the terminal web regions compared to the original confocal images (*data not shown*), the sum of intensity of both regions in the original and deblurred images remained constant and the relationship between the quantity of F-actin in the perijunctional actin-myosin ring and terminal web was the same for all agents.

### Electrical Measurements

Transepithelial electrical resistance (TER) and transepithelial dilution potential were measured across monolayers grown on permeable supports (Anocell) and mounted in an Ussing chamber at 37°C using silver/silver-chloride electrodes connected to the chamber by 3 M KCl agar bridges. Voltage and resistance were measured with a voltage clamp (model DVC-1000, World Precision Instruments, Sarasota, FL). The TER and dilution potential of bare filters in bicarbonate buffer were subtracted from all measurement with cells. For dilution potential measurements, control solutions were switched rapidly to a solution in which NaCl was replaced by raffinose. The reference electrode was placed on the basolateral side.

### Statistics

Data are presented as mean ± SE. Statistical significance was determined using the paired and unpaired *t* test and ANOVA. A $P$ value < 0.05 was considered significant.

## Results

Because we utilized a method to measure the Na flux through a localized region of tight junction and adjacent lateral intercellular space, it was possible to study the regulation of TJ Na permeability of MDCK cells independent of changes in cell membrane permeability. The strategy was to measure the Na flux across the same TJ before and after treating the monolayers with agents that are thought to change TJ permeability.

### Effect of Glucose on Na Flux Across the TJ of MDCK Cells

In the first series of experiments we studied the effect of glucose on the Na flux across the TJ of MDCK cells. For control measurements, the perfusion solution with 5

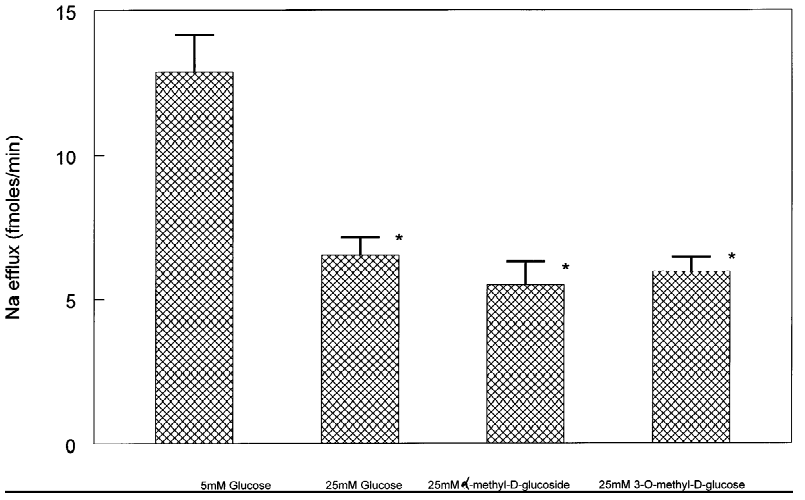


**Fig. 1.** Effect of 25 mM glucose and glucose analogues on Na efflux (mean ± SEM) across the TJ of MDCK cells. *indicates a significant decrease of Na efflux compared to control with 5 mM glucose ($P < 0.001$); the effluxes did not differ significantly between glucose and the glucose analogues.

mM glucose and high (130 mM) Na concentration was rapidly switched to one with low Na (24 mM) in which Na was replaced isomotically by Li. Acquisition of images was performed every 20 sec over a 3 min period at one focal plane in the middle of the LIS. The rate of Na efflux from the LIS was previously shown to be a measure of the Na permeability of the TJ (Kovbasnjuk et al., 1995). The flux of Na out of the LIS through the TJ was calculated from the time constant for Na efflux and previously determined LIS Na concentration (Kovbasnjuk et al., 1995; Chatton & Spring, 1995). Upon completion of the control measurements, the perfusate was switched to an isotonic solution (130 mM Na) containing 25 mM glucose. After an equilibration time (about 10 min), the solution with high Na was switched to one with low Na plus 25 mM glucose and images of the same LIS at the same focal plane were obtained. As shown in Fig. 1, 25 mM glucose significantly ($P < 0.05$) decreased the Na flux through the TJ of MDCK cells by about 50%. When 25 mM of the trisaccharide raffinose—an impermeant sugar—was added in place of the glucose, the Na flux was indistinguishable from control (*see* Fig. 3).

Experiments were performed to determine the Na efflux through the TJ as a function of glucose concentration (Fig. 2) with raffinose added to maintain an isomolar solution. The transjunctional Na efflux was not affected by a change in the perfusate glucose from 0 to 5 mM, but additional increases in glucose concentration significantly diminished the Na fluxes across the TJ.

To test whether the glucose effect on TJ Na permeability was specific, we used two glucose analogues: (1) α-methyl-D-glucoside—an analogue that shares the Na-dependent D-glucose transporter; (2) 3-O-methyl-D-glucose—an analogue that is not metabolizable and not taken up with Na in kidney (Turner & Silverman, 1977). Perfusion of MDCK monolayers with 25 mM α-methyl-D-glucoside or 25 mM 3-O-methyl-D-glucose showed the same reduction of Na efflux from LIS as was seen with

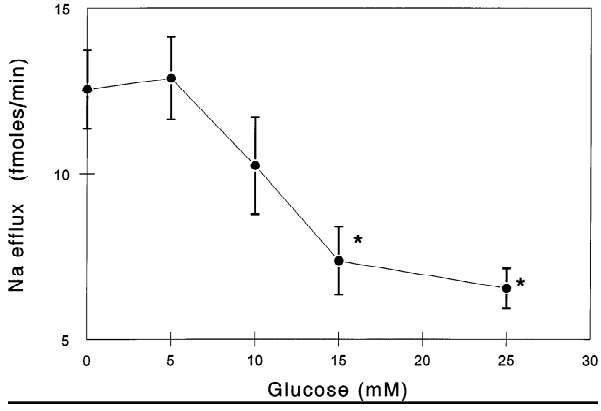


**Fig. 2.** Na efflux (mean ± SEM) across the TJ in the presence of different glucose concentrations. There was no difference in Na flux when the glucose concentration was reduced from the control value of 5 mM to 0. *indicates that increases in glucose concentration to 15 mM or 25 mM significantly ($P < 0.001$) decreased the transjunctional Na flux.

25 mM glucose (Fig. 1). We conclude that the glucose effect on TJ Na permeability is nonspecific.

Glucose entry into the cells should increase cell solute content and, therefore, cell volume. If 25 mM glucose entered the cells, the calculated cell volume increase would be about 8%, an undetectably small change with our imaging system. We hypothesized that this modest glucose-induced cell swelling could cause the observed decrease in TJ Na permeability rather than a specific effect of the sugar. To test this possibility, we added 25 mM raffinose to produce a hypertonic perfusate that is predicted to result in ~8% cell shrinkage thereby counteracting the postulated swelling effect of glucose. As shown in Fig. 3, perfusion of the cells with 25 mM glucose plus 25 mM raffinose for 10 min significantly increased the Na efflux across the TJ but did not completely restore TJ Na permeability to control levels. As expected, the Na efflux in the presence of an isotonic

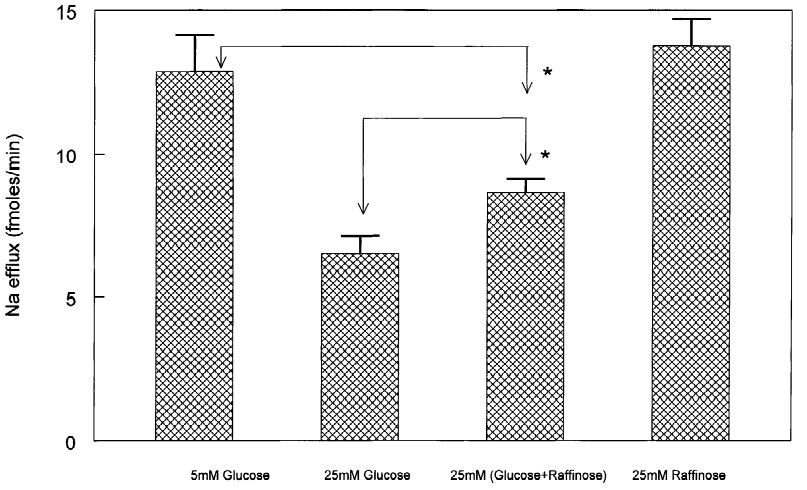


**Fig. 3.** Effect of small osmolarity changes on MDCK TJ Na permeability. Perfusion of MDCK monolayers with 25 mM glucose plus raffinose (osmolality 329–336 mOsm/kg) significantly increased ($P < 0.02$) Na efflux through the TJ compared to that with 25 mM glucose alone (osmolality 292–298 mOsm/kg). However, Na efflux in the presence of glucose plus raffinose was still significantly lower ($P < 0.02$) than that in control with 5 mM glucose. 25 mM raffinose alone (osmolality 292–298 mOsm/kg) did not alter Na efflux through the TJ compared to control.

**Table 1.** Effect of Cytochalasin D and cAMP analogues on TJ Na

Permeability of MDCK monolayers

| Condition | $J_{Na}$ (fmoles/min) | *n* | *P* |
|---|---|---|---|
| 142 mM Na + 5 mM glucose (control) | 14.38 ± 0.76 | 9 | — |
| 142 mM Na + 0.3 μM cytochalasin D | 15.56 ± 1.30 | 9 | NS |
| 130 mM Na + 25 mM glucose + 0.3 μM cyt D | 14.49 ± 1.32 | 6 | NS |
| 142 mM Na + 0.1 mM Rp-cAMPS | 7.36 ± 0.79 | 6 | <0.001 |
| 142 mM Na + 0.01 mM Sp-cAMPS | 19.59 ± 1.90 | 6 | <0.02 |
| 142 mM Na + 0.1 mM Rp-cAMPS + 0.3 μM cyt D | 7.83 ± 0.69 | 6 | <0.001 |
| 142 mM Na + 0.01 mM Sp-cAMPS + 0.3 μM cyt D | 21.33 ± 2.11 | 6 | <0.005 |

solution containing 25 mM raffinose in place of glucose did not significantly change junctional Na permeability compared to control (Fig. 3).

### Effect of Cytochalasin on TJ Permeability

As previously described (Madara, 1991), intestinal epithelial junctional complexes have associations with cytoskeletal components that could mediate changes in TJ structure and permeability. Cytochalasin D, which disrupts F-actin microfilaments, decreased intestinal epithelial (T84) monolayer electrical resistance, presumably due to a disruptive effect on the perijunctional actin-myosin ring (Madara et al., 1988). To determine the usefulness of cytochalasin D as a tool to study the role of the cytoskeleton in the regulation of TJ Na permeability of MDCK cells, we perfused monolayers for about 10 min with 1.8 μM cytochalasin D, a concentration used by Madara et al. (1988). This dose dramatically changed the shape of cells during the experimental period, and we concluded that the concentration was too high for MDCK cells. We subsequently determined that a concentration of 0.3 μM cytochalasin D did not cause visible changes of cell geometry. Perfusion of MDCK monolayers with this concentration of cytochalasin D for 10 min also did not alter the Na flux across the TJ (Table 1).

When cells were treated with 0.3 μM cytochalasin D and 25 mM glucose simultaneously, the effect of glucose to reduce Na permeability of the TJ was completely blocked. The resultant Na flux across the TJ did not differ from the control value with low glucose (Table 1) and was significantly increased compared to 25 mM glucose alone. Thus, an intact cytoskeleton was essential for manifestation of the effect of glucose on TJ permeability. A similar result was obtained by Stevenson and Begg (1994) in which the increased TJ permeability of MDCK cells associated with calcium chelation was prevented by cytochalasin D treatment.

We recently reported that the cAMP analogues, Rp-cAMPS—an inhibitor of protein kinase A (PKA) and Sp-cAMPS—an activator of PKA, altered the junctional tightness of MDCK cells (Kovbasnjuk et al., 1995). Stimulation of PKA significantly increased TJ Na permeability while inhibition of PKA diminished it. Since 0.3 μM cytochalasin D abolished the effect of high glucose concentration on Na flux through the TJ, we tested whether cytochalasin D also blocked the influence of PKA activity on TJ permeability.

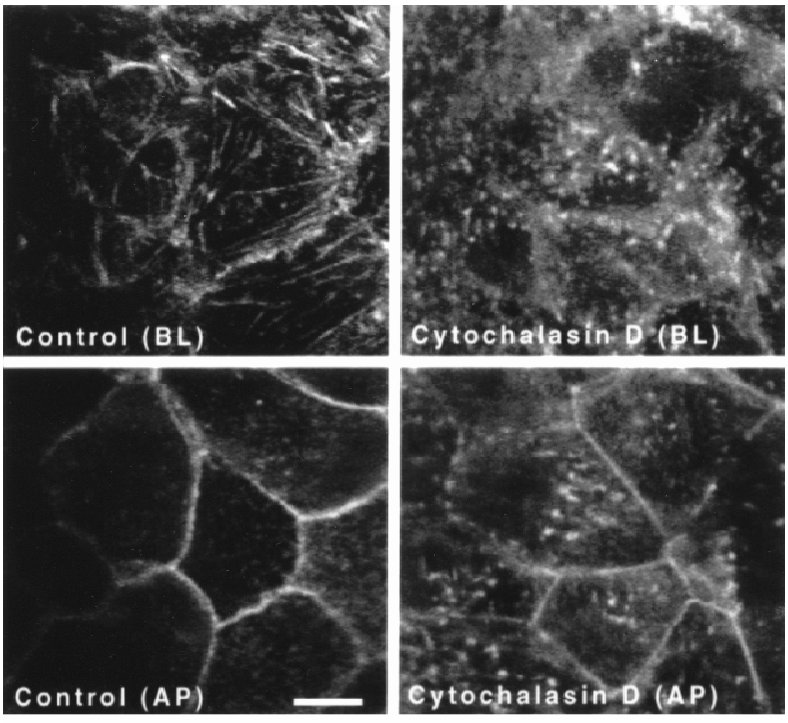


4

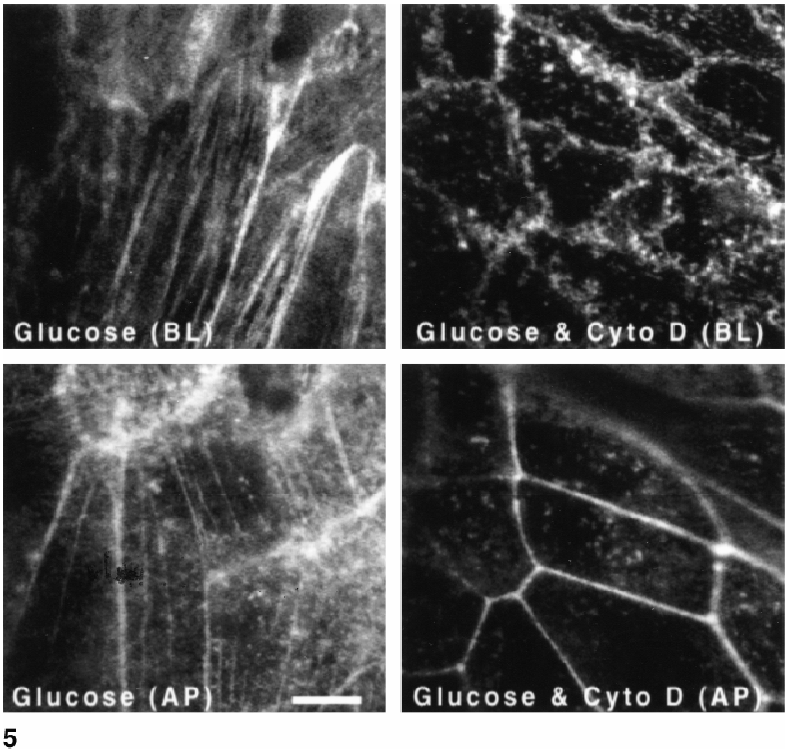


5

**Fig. 4–6.** Confocal fluorescence images showing the distribution of MDCK cell actin filaments in control conditions and in monolayers treated with cytochalasin D, glucose, Sp-cAMPS or Rp-cAMPS. (AP) indicates the optical section was at the level of the TJ, and (BL) indicates the section was at the basal level. Confluent monolayers of MDCK cells were grown on glass coverslips and fixed in formaldehyde as described in methods. F-actin was labeled with Oregon-Green-488-phalloidin. Scale bar indicates 5 μm.

We first repeated our previous experiments with 0.1 mM Rp-cAMPS or 0.01 mM Sp-cAMPS to ensure that response of the cells in the present study did not differ from those used before. The effects of the cAMP analogues on Na efflux across the TJ were indistinguishable from those published before. Perfusion of MDCK monolayers with 0.3 μM cytochalasin D and 0.1 mM Rp-cAMPS or 0.01 mM Sp-cAMPS showed that cytochalasin D did not alter the effects of either agent on TJ permeability (Table 1). Thus, the actions of these cAMP

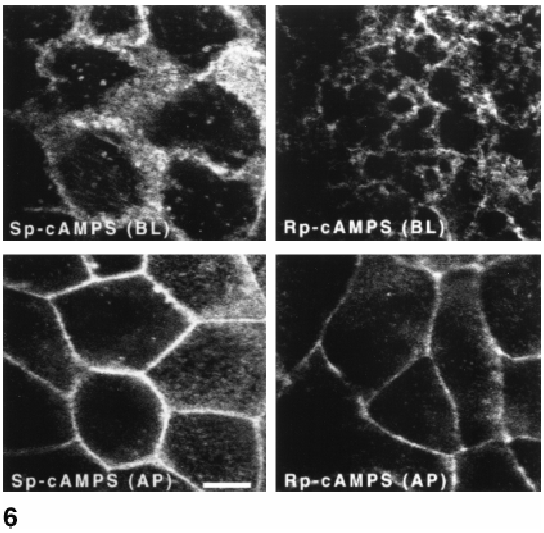


6

**Fig. 6.** Continued

analogues on TJ permeability were not dependent on an intact cytoskeleton.

### F-ACTIN DISTRIBUTION IN MDCK CELLS

To ascertain whether a relationship existed between junctional tightness and the cytoskeleton, we examined the distribution of actin filaments after incubation of MDCK monolayers with the agents mentioned above that alter TJ Na permeability. Ten monolayers were examined for each treatment, and the results presented are representative of the majority (~60–75%) of the cells in the monolayers. Optical sections of MDCK cells done by confocal fluorescence microscopy (Fig. 4, control) demonstrate two distinct populations of actin filaments: (1) large fiber bundles present on the basal side of monolayers, (2) smaller fibers in the terminal web and actin peripheral ring at the level of the TJ. Figure 4 shows the disruption in F-actin organization of MDCK cells caused by treating monolayers with 0.3 μM cytochalasin D, a dose that caused no significant change in TJ permeability. At the basal focal plane of monolayers exposed to cytochalasin D, actin appears as irregularly distributed brightly fluorescent aggregates. At the apical level, F-actin staining is somewhat irregular at the perijunctional ring with brightly fluorescent intracellular aggregates. The F-actin staining was not altered by perfusion with the low Na bathing solution that was required for the TJ Na permeability measurements (*data not shown*).

Incubation of MDCK cells with 25 mM glucose resulted in the formation of long thin F-actin threads on both apical and basal surface compared to control (Fig. 5); incubation with 25 mM raffinose in place of glucose had no discernable effect on F-actin distribution (*data not shown*). In cells treated with cytochalasin D and glucose simultaneously (Fig. 5), F-actin distribution on both basal and apical levels resembled that in the case of cytochalasin alone except for a more continuous ring in cell borders.

Examination of the F-actin distribution in monolayers incubated with 0.01 mM Sp-cAMPS or 0.1 mM Rp-cAMPS showed a narrow brightly fluorescent ring around the cells at the tight junctional focal plane that was similar to that under control conditions (Fig. 6). However, on the basal level of the cells, Sp-cAMPS treatment lead to the formation of a wide discontinuous ring in the cell border and irregularly distributed intracellular aggregates. In the case of Rp-cAMPS, most of the basal surface of MDCK cells revealed circular structures with bright staining that were interconnected and organized into a net (Fig. 6).

### F-ACTIN QUANTITATION

Because of our interest in any possible connections between the cytoskeleton and TJ permeability, we directed our attention to the cell's apical pole. Two mechanisms could be involved in the observed reorganization of actin filaments at the apical end of the cell: (1) redistribution of F-actin between the perijunctional ring and the terminal web or (2) polymerization-depolymerization reactions. To quantitate the changes in actin distribution, we selected confocal fluorescence images at the tight junctional level and generated two masks for each cell—one to demarcate the perijunctional F-actin ring around the cell and one the terminal web area underlying the apical membrane. The intensity of fluorescence, corresponding to the quantity of F-actin, was measured in each region.

As shown in Fig. 7, the quantity of F-actin in the two designated regions of the apical pole of the cells was not significantly changed by treatment with cAMP analogues compared to control although there were significant differences between the total quantity of F-actin in Sp-cAMPS and Rp-cAMPS treated tissues. We conclude that changes in PKA activity result in reorganization of the MDCK cell cytoskeleton rather than redistribution of F-actin between the intracellular space and perijunctional ring or polymerization-depolymerization reactions. In contrast, incubation of monolayers with 25 mM glucose lead to a reduction of the quantity of F-actin in both regions.

As expected, there was a substantial decrease in the total quantity of actin filaments under all conditions after treatment with cytochalasin D (Fig. 7). Cytochalasin D further reduced the quantity of F-actin in tissues exposed to 25 mM glucose to nearly the same levels as in the cells treated with cytochalasin D alone. Cytochalasin D also decreased the total quantity of F-actin in tissues treated with Rp-cAMPS.

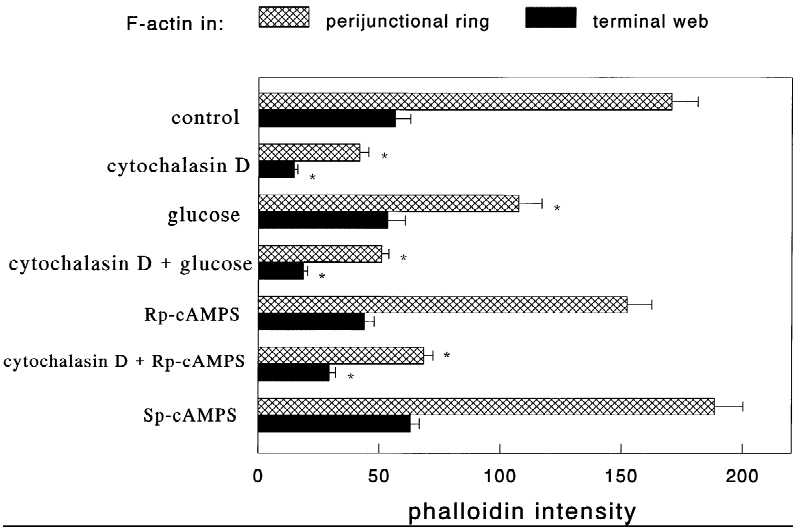


**Fig. 7.** The integrated intensity of the fluorescence of Oregon-Green-488-phalloidin corresponding to the amount of polymerized actin filaments in two regions of MDCK cells treated with agents that were used to alter TJ Na permeability. The phalloidin intensity (mean ± SEM) for 10 independent measurements in each experimental condition were as follows: (the first value is the intensity in perijunctional ring and the second is that in the terminal web region): control 170.41 ± 10.82, 56.4 ± 6.35; cytochalasin D 41.76 ± 3.71, 14.08 ± 1.46; glucose 107.39 ± 9.6, 53.32 ± 7.32; cytochalasin D + glucose 50.95 ± 2.93, 18.71 ± 1.67; Rp-cAMPS 152.32 ± 10.1, 43.81 ± 4.11; cytochalasin D + Rp-cAMPS 68.46 ± 3.77, 29.41 ± 2.59; Sp-cAMPS 188.39 ± 11.73, 62.95 ± 3.79. *indicates a significant change in the quantity of F-actin compared to control ($P < 0.05$).

A plot of the quantity of F-actin in the terminal web *vs.* F-actin in the perijunctional ring for all experimental conditions (Fig. 8) shows that all agents, except glucose, changed the quantity of actin filaments in both regions proportionately. Exposure to Sp-cAMPS significantly increased the quantity of F-actin computed to experiments with Rp-cAMPS or glucose. However, glucose addition decreased perijunctional F-actin significantly ($P < 0.05$) more than expected from the observed decrease in terminal web F-actin. The decreases in F-actin in both regions caused by cytochalasin D alone, or in combination with other agents, were highly correlated ($r = 0.93$; $P < 0.001$). These results support the idea that the low dose of cytochalasin D decreases the quantity of actin filaments by disruption rather than by redistribution.

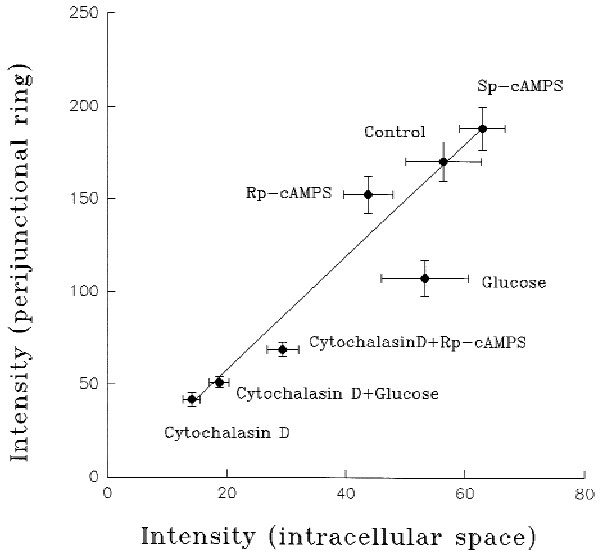


**Fig. 8.** Distribution of MDCK cell actin filaments between intracellular space and perijunctional ring at the terminal web level. All agents tested changed the amount of F-actin in both regions by an approximately equal extent.

## Relationship Between TJ Permeability and F-actin

A plot of the Na flux through the TJ *vs.* the quantity of F-actin in the perijunctional ring revealed an apparent correlation (Fig. 9). The increase in TJ Na permeability during perfusion of monolayers with Sp-cAMPS coincided with the increase in quantity of F-actin in both regions. Reduction of Na efflux through the TJ caused by treating of cells with Rp-cAMPS or glucose correlated with a decrease of the total quantity of F-actin. Of course, this correlation no longer held when the tissue is treated with cytochalasin D.

## Transepithelial Electrical Resistance Measurements

The most widely used method for the measurement of changes in the paracellular permeability of epithelia is the TER. Since we observed both up- and downregulation of the Na permeability of MDCK cell TJ of cells grown on glass coverslips, it was of interest to compare the TER of cells grown on permeable supports. The value of the TER under control conditions (Table 2) is in good agreement with measurements for the low resistance strain of MDCK cells made by other investigators (Barker & Simmons, 1981; Balda et al., 1996). Perfusion of MDCK cells with 25 mM glucose or 0.1 mM Rp-cAMPS for 10–20 min, both treatments that substantially decreased the Na flux through the TJ of cells grown on glass coverslips, did not significantly alter the TER of cells grown on permeable supports (Table 2). In contrast, 0.01 mM Sp-cAMPS, an agent that nearly doubled TJ Na permeability of cells on glass, led to a 50% de-

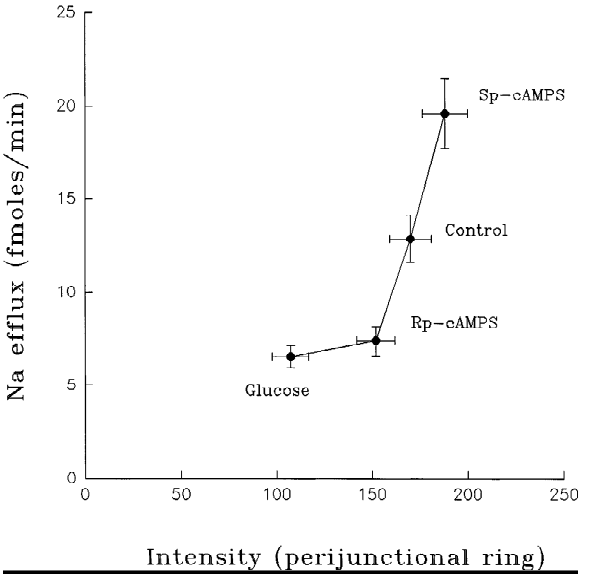


**Fig. 9.** Relationship between the amount of F-actin in the perijunctional ring of MDCK cells treated with glucose or cAMP analogues and the magnitude of the Na efflux across the TJ. The intensity of F-actin staining in the perijunctional ring differed significantly between all points except that Rp-cAMPS and Sp-cAMPS did not differ from control although they were different from one another. A higher quantity of F-actin correlated with greater TJ Na permeability.

**Table 2.** Transepithelial electrical resistance of MDCK monolayers

| Condition | TER ($\Omega$* cm$^2$) | *n* | *P* |
|---|---|---|---|
| 142 mM Na + 5 mM glucose (control) | 65.0 ± 9.6 | 9 | — |
| 130 mM Na + 25 mM glucose | 65.0 ± 5.2 | 12 | NS |
| 142 mM Na + 0.3 μM cytochalasin D | 39.5 ± 5.5 | 11 | <0.05 |
| 142 mM Na + 0.1 mM Rp-cAMPS | 62.6 ± 13.2 | 9 | NS |
| 142 mM Na + 0.01 mM Sp-cAMPS | 31.1 ± 5.3 | 11 | <0.05 |

crease in TER compared to control. Although 0.3 μM cytochalasin D did not significantly change junctional Na permeability of cells on glass, the TER of monolayers decreased significantly when they were treated with this concentration for 10 min. Thus, only in the case of Sp-cAMPS treatment was there any correlation between the direct measurements of TJ Na permeability of cells grown on glass coverslips and the TER of cells grown on permeable supports.

### Dilution Potential Measurements

Because treatment of MDCK monolayers with glucose or Rp-cAMPS did not change the TER of cells grown on permeable supports while both significantly decreased TJ Na permeability of cells grown on glass coverslips, we were concerned that these agents might have caused a simultaneous offsetting increase in epithelial Cl permeability that would result in no detectable change in TER. Therefore, the Na *vs.* Cl selectivity of the paracellular pathway of the monolayers was determined from the transepithelial dilution potential developed when the NaCl concentration of one bathing solution was reduced about sixfold. The apical solution with high (142 mM or 130 mM) Na concentration was switched rapidly to a solution in which 118 mM or 106 mM NaCl was replaced by raffinose. The dilution potential average for control measurements was 27.1 ± 1.3 mV (6 monolayers), basolateral solution negative. Such a NaCl dilution potential is consistent with a cation-selective tight junction with a Na transference number of 0.86. The high Na selectivity is in agreement with our previous data (Kovbasnjuk et al., 1995) and slightly higher than the value for MDCK cells of 0.64 reported by other investigators (Oberleithner, Vogel & Kersting, 1990). Perfusion of monolayers with solution containing 25 mM glucose or 0.1 mM Rp-cAMPS did not alter the value of the dilution potential compared to control (*data not shown*). Transepithelial dilution potential measurements demonstrate that neither glucose nor Rp-cAMPS changed the ratio of Na and Cl permeability across MDCK cell monolayers. Thus, changes in ionic selectivity of the tight junctions could not be the cause of discrepancy between the transjunctional Na permeability and TER data.

## Discussion

We applied our method (Kovbasnjuk et al., 1995; Chatton & Spring, 1995) for the direct measurement of the transjunctional flux of Na in MDCK epithelium to study the regulation of TJ Na permeability. We demonstrated that glucose and its analogues lead to downregulation of TJ Na permeability and showed that the glucose effect was dependent on an intact cytoskeleton. In contrast, the changes in TJ Na permeability caused by treatment with cAMP analogues were unaffected by the disruption of F-actin. We also determined the amount of phalloidin-labeled F-actin in the perijunctional ring and terminal web regions of the cell and observed that the amount of F-actin in the perijunctional ring correlated with the TJ Na permeability.

### Effect of Glucose on TJ Na Permeability

It was previously reported that glucose increased the paracellular sodium or mannitol permeability of small intestinal epithelium (Madara & Pappenheimer, 1987; Atisook et al., 1990). The same glucose concentration used on small intestine caused the opposite effect on MDCK epithelial cells—Na efflux across the TJ signifi-

cantly decreased. Treatment of MDCK monolayers with two glucose analogues, α-methyl-D-glucoside and 3-O-methyl-D-glucose, showed identical decreases of transjunctional Na permeability as in experiments with glucose. MDCK cells, unlike those of the small intestinal epithelium, do not express the Na-D-glucose cotransporter (Pascoe et al., 1996), therefore sugar transport into MDCK cells is Na-independent. Because both glucose and its analogues showed the same effect on Na efflux across the TJ, we concluded that the glucose effect was nonspecific. We hypothesized that the entry of glucose or its analogue into the cells via facilitated diffusion would cause an immeasurably small (i.e., 8%) cell swelling that could alter the cytoskeleton and thereby reduce TJ permeability. We reasoned that treatment of the cells with a slightly hypertonic solution, containing 25 mM raffinose (an impermeant sugar) and 25 mM glucose simultaneously, should offset the effect of glucose alone on cell volume and return the TJ Na permeability to the control level. Our results showed that, although the added raffinose increased the Na efflux across the TJ by 33%, permeability was not restored to control levels. One possibility is that exposure to a hypertonic solution may itself have other effects on the cytoskeleton (Mills et al., 1994) that further complicate interpretation of the experiment.

### Cytoskeleton Involvement in the Regulation of TJ Na Permeability

Since it has been proposed that TJ permeability is controlled by the cytoskeleton in small intestine, we studied the distribution of actin filaments to determine whether glucose or PKA altered F-actin polymerization. Madara and Pappenheimer (1987) showed that apical membrane Na-coupled transport of glucose into small intestine cells triggered a contraction of the actin filaments associated with the junctional complex coincident with the increase in TJ permeability. Cytochalasin D and B, both of which disrupt actin organization within small intestine cells, also resulted in a decrease of paracellular resistance and alterations in the organization of the junctional fibrils (Meza et al., 1980; Madara et al., 1987).

We found that exposure of MDCK monolayers to a low dose of cytochalasin D, one that did not disturb the shape of cells, lead to significant changes in distribution of actin filaments, but not to changes in TJ Na permeability. We also observed that this low dose of cytochalasin blocked the reduction in Na permeability of the TJ caused by increased glucose but failed to influence the permeability changes associated with PKA stimulation or inhibition. It is worthy of note that PKA stimulation or inhibition resulted both in changes of the total quantity of F-actin in the apical region of MDCK cells and in dramatic alterations in F-actin distribution at the basal region of the cells. These results are consistent with the conclusion that the cytoskeleton is involved only in the glucose-induced changes in TJ Na permeability.

Our experiments also demonstrated an apparent correlation between the amount of F-actin in the perijunctional ring and the Na permeability of the TJ, with more F-actin coinciding with a higher TJ Na permeability. Other investigators (Hecht et al., 1996; Gandhi, Lorimer & de Lanerolle, 1997) have also reported increases in MDCK paracellular permeability after increased stiffening of the cytoskeleton by expression of the catalytic domain of myosin light chain kinase. Thus stiffening of the cytoskeleton, by increased F-actin in the perijunctional ring or by other means, may be associated with a loosening of the tight junctions, and decreases in perijunctional F-actin may lead to tightening of the junctions. However, our results with cytochalasin D do not fit this pattern as TJ Na permeability remained at control levels (Table 1) while perijunctional F-actin decreased markedly (Fig. 7). We speculate that cytochalasin D treatment is sufficiently disruptive to render suspect any interpretation of the structure-function relationship of the cytoskeleton and tight junctions.

It has not been unequivocally established in our experiments, or those of others, that the observed changes in F-actin are causally related to the alterations in TJ permeability. The requisite experimental evidence will probably come from studies of the molecular interactions of cytoskeletal and tight junctional proteins rather than from the structure-function correlations utilized in this study. Indeed, while our results offer support for a direct role of the cytoskeleton in alterations of MDCK cell tight junctions, the detailed nature of this interaction remains to be established.

### Transjunctional Permeability and TER

Our method for measurement of Na efflux across individual tight junctions enabled a comparison of the TJ Na permeability of cells grown on glass coverslips and that estimated from the TER of monolayers grown on permeable supports. This comparison revealed a poor correlation between these two measures. The TJ Na flux technique was limited to cells grown on glass coverslips and determination of TER requires that the monolayers be grown on permeable supports. While it would have been preferable to measure the TJ Na permeability of cells grown on permeable supports, we have not yet developed the methodology for such measurements.

For many years, TER measurements have been used as a simple indicator of the transjunctional permeability of epithelia as the TER is proportional to the average tissue permeability to inorganic ions. It was shown previously (Gonzalez-Mariscal et al., 1989) that changes in TER of MDCK monolayers primarily reflect changes in

the resistance of paracellular pathway. TER between lumen and blood side of renal tubules increases from the proximal to the distal tubule more or less in proportion to the number of strands in the TJ (Claude & Goodenough, 1973). However this correlation is far from universal. For example, two distinct strains of MDCK cells have similar numbers of TJ strands but display a huge difference in TER (Barker & Simmons, 1981; Stevenson et al., 1988). Although a reduction in temperature increased the TER of MDCK cell monolayers more than threefold, the structure of the TJ by freeze fracture was unaffected (Gonzalez-Mariscal et al., 1984). Recently, a substantial discrepancy between the paracellular permeability to tracers and the electrical tightness of the epithelium was found when the expression of COOH-terminally truncated chicken occludin (the only known transmembrane component of the TJ) in MDCK cells produced both an increase in TER and a paradoxical severalfold increase in the paracellular flux of small molecular weight tracers (Balda et al., 1996). TER and related methods used to determine paracellular permeability (e.g., permeation of electron dense, fluorescent or radioactive tracers) assess the entire epithelium and are subject to errors arising from cellular heterogeneity, or leaks across damaged or desquamated areas.

TER for the low resistance strain of MDCK cells in our control experiments was about 65 $\Omega \cdot cm^2$, in good agreement with previous measurements (Barker & Simmons, 1981; Stevenson et al., 1988; Balda et al., 1996). Comparison of our TER and TJ Na flux data demonstrate that only in case of Sp-cAMPS did the increase of Na efflux across the TJ correlate with the decrease in electrical resistance. Otherwise, there was a contradiction in the estimation of transjunctional permeability by these two methods. The discrepancy between the TER and the observed decreases in TJ Na flux could have been the result of compensatory increases in TJ Cl permeability. Dilution potential experiments demonstrated that this was not the case. We also repeated the cytoskeleton staining experiments on cells grown on permeable supports and observed the same patterns of F-actin distribution as was seen in cells grown on glass coverslips, ruling out the possibility that the agents used were ineffective when the cells had access to both bathing solutions (*data not shown*). We conclude that TER of cells grown on permeable supports is not a reliable indicator of the tight junctional permeability of cells grown on a solid substrate. A direct comparison of these two measures will have to await adaptation of the technique for the measurement of TJ Na permeability to cells grown on permeable supports.

In summary, regulation of the Na permeability of the MDCK cell tight junction appears to occur by at least two mechanisms: (1) through an action of PKA independent of the cytoskeleton, and (2) by alterations in the amount of F-actin in the perijunctional actin-myosin ring. The effect of glucose and related sugars to decrease MDCK cell tight junctional Na permeability requires an intact cytoskeleton and may be a consequence of the cell volume changes caused by solute uptake rather than a specific effect of the sugar. While a correlation exists between the amount of F-actin in the perijunctional ring and the TJ Na permeability, a cause and effect relationship between these two variables has yet to be proven.

## References


Anderson, J.M., van Itallie, C.M. 1995. Tight junctions and the molecular basis for regulation of paracellular permeability. *Am. J. Physiol.* **269:**G467–G475

Atisook, K., Carlson, S., Madara, J.L. 1990. Effects of phlorizin and sodium on glucose-elicited alterations of cell junctions in intestinal epithelia. *Am. J. Physiol.* **258:**C77–C85

Bakker, R., Groot, J.A. 1984. cAMP-mediated effects of ouabain and theophylline on paracellular ion selectivity. *Am. J. Physiol.* **246:**G213–G217

Bakker, R., Groot, J.A. 1989. Further evidence for the regulation of the tight junction ion selectivity by cAMP in goldfish intestinal mucosa. *J. Membrane Biol.* **111:**25–35

Balda, M.S. 1992. Intracellular signals in the assembly and sealing of tight junctions. *In:* Tight Junctions. M. Cereijido, editor. pp. 121–137. CRC Press, Boca Raton, FL

Balda, M.S., Whitney, J.A., Flores, C., Gonzalez, S., Cereijido, M., Matter, K. 1996. Functional dissociation of paracellular permeability and transepithelial electrical resistance and disruption of the apical-basolateral intramembrane diffusion barrier by expression of a mutant tight junction membrane protein. *J. Cell Biol.* **134:**1031–1049

Balda, M.S., Gonzalez-Mariscal, L., Contreras, R.G., Macias-Silva, M., Torres-Marquez, M.E., Garcia Sainz, J.A., Cereijido, M.M. 1991. Assembly and sealing of tight junctions: possible participation of G-proteins, phospholipase C, protein kinase C and calmodulin. *J. Membrane Biol.* **122:**193–202

Barker, G., Simmons, N.L. 1981. Identification of two strains of cultured canine renal epithelial cells (MDCK cells) which display entirely different physiological properties. *Q.J. Exp. Physiol.* **66:**61–72

Cereijido, M. 1992. Evolution of ideas on the tight junction. *In:* Tight Junctions. M. Cereijido, editor. pp. 1–13. CRC Press, Boca Raton, FL

Chatton, J.-Y., Spring, K.R. 1995. The sodium concentration of the lateral intercellular spaces of MDCK cells: a microspectrofluorimetric study. *J. Membrane Biol.* **144:**11–19

Chatton, J.-Y., Spring, K.R. 1993. Light sources and wavelength selection for widefield fluorescence microscopy. *MSA Bull.* **23:**324–333

Claude, P. 1978. Morphological factors influencing transepithelial permeability: a model for the resistance of the zonula occludens. *J. Membrane Biol.* **39:**219–232

Claude, P., Goodenough, D.A. 1973. Fracture faces of zonulae occludentes from ''tight'' and ''leaky'' epithelia. *J. Cell Biol.* **58:**390–400

Diamond, J.M. 1977. The epithelial junction: bridge, gate and fence. *Physiologist* **20:**10–18

Duffey, M.E., Hainan, B., Ho, S., Bentzel, C.J. 1981. Regulation of the epithelial tight junction permeability by cyclic AMP. *Nature* **294:**451–453

Gandhi, S., Lorimer, D.D., de Lanerolle, P. 1977. Expression of a mutant myosin light chain that cannot be phosphorylated increases paracellular permeability. *Am. J. Physiol.* **272:**F214–F221

Gonzalez-Mariscal, L.B., Chavez de Ramirez, Lazaro, A., Cereijido, M. 1989. Establishment of tight junctions between cells from different animal species and different sealing capacities. *J. Membrane Biol.* **107:**43–56

Gonzalez-Mariscal, L.B., Chavez de Ramirez, B., Cereijido, M. 1984. Effect of temperature on the occluding junctions of monolayers of epitheloid cells (MDCK). *J. Membrane Biol.* **79:**175–184

Gumbiner, B. 1987. The structure, biochemistry and assembly of epithelial tight junctions. *Am. J. Physiol.* **253:**C749–C758

Harris, P.J., Chatton, J.-Y., Tran, P.H., Bungay, P.M., Spring, K.R. 1994. Optical microscopic determination of pH, solute distribution and diffusion coefficient in the lateral intercellular spaces of epithelial cell monolayers. *Am. J. Physiol.* **266:**C73–C80

Hecht, G.C., Pestic, L., Nikcevic, G., Koytsoyris, A., Tripuraneni, J., Lorimer, D.D., Nowak, G., Guerriero, V., Elson, E., de Lanerolle, P. 1996. Expression of the catalytic domain of myosin light chain kinase increases paracellular permeability. *Am. J. Physiol.* **271:**C1678–C1684

Holman, G.D., Naftalin, R.J., Simmons, N.L., Walker, M. 1979. Electrophysiological and electron-microscopical correlations with fluid and electrolyte secretion in rabbit ileum. *J. Physiol.* **290:**367–386

Kottra, G., Haase, W., Frömter, E. 1993. Tight-junction tightness of *Necturus* gall bladder epithelium is not regulated by cAMP or intracellular $Ca^{2+}$ I. Microscopic and general electrophysiological observations. *Pfluegers Arch.* **425:**528–534

Kottra, G., Frömter, E., 1993. Tight-junction tightness of *Necturus* gall bladder epithelium is not regulated by cAMP or intracellular $Ca^{2+}$ II. Impedance measurements. *Pfluegers Arch.* **425:**535–545

Kovbasnjuk, O., Chatton, J.-Y., Friauf, W.S., Spring, K.R. 1995. Determination of the Na permeability of the tight junctions of MDCK cells by fluorescence microscopy. *J. Membrane Biol.* **148:**223–232

Madara, J.L. 1991. Relationships between the tight junction and the cytoskeleton. *In:* Tight junctions. M. Cereijido, editor. pp. 105–119. CRC Press, Boca Raton, FL

Madara, J.L., Stafford, J., Barenberg, D., Carlson, S. 1988. Functional coupling of tight coupling of tight junctions and microfilaments in T84 monolayers. *Am. J. Physiol.* **254:**G416–G423

Madara, J.L. 1987. Intestinal absorptive cell tight junctions are linked to cytoskeleton. *Am. J. Physiol.* **253:**C171–C175

Madara, J.L., Pappenheimer, J.R. 1987. Structural basis for physiological regulation of paracellular pathways in intestinal epithelia. *J. Membrane Biol.* **100:**149–164

Meza, I., Ibarra, G., Sabenero, M., Martinez-Palomo, M., Cereijido, M. 1980. Occluding junctions and cytoskeletal components in a cultured transporting epithelium. *J. Cell Biol.* **87:**746–754

Mills, J.W., Lubin, M. 1986. Effect of adenosine 3′,5′-cyclic monophosphate on volume and cytoskeleton of MDCK cells. *Am. J. Physiol.* **250:**C319–C324

Oberleithner, H., Vogel, U., Kersting, U. 1990. Madin-Darby canine kidney cells. I. Aldosterone-induced domes and their evaluation as a model system. *Pfluegers Arch.* **416:**526–532

Pascoe, W.S., Inukai, K., Oka, Y., Slot, J.W., James, D.E. 1996. Differential targeting of facilitative glucose transporters in polarized epithelial cells. *Am. J. Physiol.* **271:**C547–C554

Schneeberger, E.E., Lynch, R.D. 1992. Structure, function and regulation of cellular tight junctions. *Am. J. Physiol.* **262:**L647–L661

Stevenson, B.R., Begg, D.S. 1994. Concentration-dependent effects of cytochalasin D on tight junctions and actin filaments in MDCK epithelial cells. *J. Cell Sci.* **107:**367–375

Stevenson, B.R., Anderson, J.M., Goodenough, D.A., Mooseker, M.S. 1988. Tight junction structure and ZO-1 Content are identical in two strains of Madin-Darby Canine Kidney cells which differ in transepithelial resistance. *J. Cell Biol.* **107:**2401–2408

Turner, R.J., Silverman, M. 1977. Sugar uptake into brush border vesicles from normal human kidney. *Proc. Natl. Acad. Sci.* **74:**2825–2829